High frequency hysteresis-free switching in thin layers of smectic-C^* ferroelectric liquid crystals

L. M. Blinov,[1,2,*] S. P. Palto,[1] E. P. Pozhidaev,[3,4] Yu. P. Bobylev,[3] V. M. Shoshin,[3] A. L. Andreev,[3] F. V. Podgornov,[4] and W. Haase[4]

[1]*Shubnikov Institute of Crystallography, Russian Academy of Science, Leninsky Prospect 59, 117333 Moscow, Russia*

[2]*Physics Deptartment, INFM, Calabria University, Arcavacata di Rende(Cs), Italy*

[3]*Lebedev Physical Institute, Russian Academy of Science, Leninsky Prospect 53, 119924 Moscow, Russia*

[4]*E. Zintl Institut für Anorganische und Physikalische Chemie, TUD, Petersenstrasse 20, D-64287 Darmstadt, Germany*

(Received 17 November 2004; published 27 May 2005)

The insulating layers used for the alignment of ferroelectric liquid crystals (FLC) in electro-optical cells usually have non-negligible thickness and their capacitance determines the type of the director switching caused by a triangular-form external voltage U_{tr}. With decreasing frequency of U_{tr}, the hysteresis in a switching direction changes from the normal to the abnormal one at a characteristic hysteresis inversion frequency f_i. In the vicinity of f_i, the electro-optical response is thresholdless and the optical transmission manifests the V-shape field dependence. The V-shape regime is very interesting for certain applications, in particular to microdisplays due to a possibility of the gray scale realization. However, f_i has to be enhanced from the usually observed frequency of a few Hz up to the range of hundreds of Hz. To this effect, a special FLC material has been designed and its basic properties (tilt angle, spontaneous polarization, rotational viscosity, and electric conductivity) have been measured over the entire range of the smectic-C^* phase. Upon variation of cell parameters (thickness of both the FLC and alignment layers), temperature, and external voltage, the frequency of the V-shape effect as high as 150–1000 Hz (in the temperature range 30–75 °C) has been found experimentally. The operating voltage remains lower than 8 V. A quantitative interpretation of these results has been done using the modeling procedure developed earlier [S.P. Palto, Cryst. Rep. **48**, 124 (2003)]. The modeling has been performed with the experimental values of the FLC material and the cell parameters and has shown very good agreement with experiment. The key point of this approach is consideration of the internal voltage on the FLC layer, the sign, amplitude, and form of which differ from U_{tr}. The results of the modeling allow further improvement of the performance of electro-optical FLC cells for high frequency V-shape effect.

DOI: 10.1103/PhysRevE.71.051715 PACS number(s): 61.30.Cz, 61.30.Gd, 42.79.Kr

I. INTRODUCTION

Ferroelectric liquid crystals (FLCs) have a layered chiral smectic-C^*(SmC^*) structure and possess the spontaneous polarization, which can be switched between two states by an external ac voltage [1]. When an FLC structure is stabilized by surfaces, its electro-optical switching manifests a threshold behavior with a characteristic hysteresis [2]. However, several publications deal with a so-called "V-shape" or "thresholdless" switching mode of ferroelectric and antiferroelectric liquid crystals following the pioneering work [3]. In this case, the bookshelf alignment of smectic layers is provided by fairly thick insulating films and a cell is placed between crossed polarizers with the smectic layer normal along the electric vector of the incident light. When a triangular voltage waveform is applied to such a cell, the field-induced optical transmission curve acquires a form of the letter V showing neither a threshold nor hysteresis. The V-shape regime is very interesting for applications to the projection displays and the speed of the response is a key parameter. However, usually the investigations of this phenomenon are limited by frequencies not exceeding 10 Hz, at least at room temperature.

Several mechanisms were suggested for explanation of the phenomenon in the antiferroelectric and ferroelectric phases [4–12]. In the particular case of the SmC^* phase, the most important factor determining the very existence of the V-shape mode was shown to be an increased thickness of the layers used for alignment of FLCs [7–10,12]. More precisely, the aligning layers should have small capacitance and high resistance. Then, in the close external circuit, the charge and the voltage on these insulating layers will be high enough to maintain or even invert the internal field in the FLC layer [10,12].

Recently one of us [13] has developed a software that allows the modeling of FLC electro-optical switching at arbitrary field forms on account of properties of both FLC layers and alignment layers. The software takes into account the anisotropy of the basic properties of an FLC (dielectric permittivities, elastic moduli, viscosity coefficients, and azimuthal and zenithal components of the quadrupolar-type of the FLC anchoring) and conductivity of FLC and aligning layers. The software was shown to reproduce many experimental observations, in fact without fitting parameters [12–14].

The scope of the present investigation is as follows. With our new software we have analyzed a possibility for increasing the operating frequency of the hysteresis-free switching by varying the properties of a liquid crystal material and parameters of an electro-optical cell. In experiment, we have succeeded to increase the operating frequency up to 0.1–1 kHz (depending on temperature) keeping low operating voltage and reasonable optical contrast. In the present paper, we

*Corresponding author. Email address: blinov@fis.unical.it

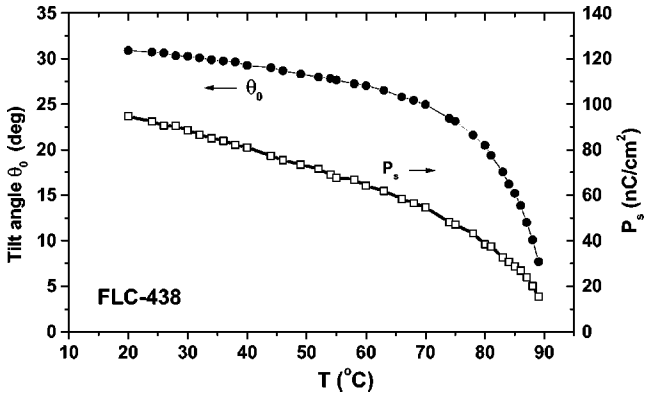

FIG. 1. Temperature dependencies of tilt angle ϑ_0 and spontaneous polarization P_s of FLC-438.

show our best experimental results and make quantitative comparison of them with the results of our modeling.

II. EXPERIMENT

A. Material and cells

1. Material

We have tested many FLC materials for the V-shape electro-optical switching at elevated frequencies. Some examples can be found in our previous publications [10,12,15,16]. The best results were obtained with a four-component mixture FLC-438 that is a combination of a three-component achiral smectic-*C* matrix (phenylpyrimidine and biphenylpyrimidine derivatives) and a chiral derivative of terphenyl-bicarboxylic acid. The temperature dependencies of the most important properties of the mixture are shown in Figs. 1 and 2. They were measured using conventional techniques using (1–2)-μm-thick cells with *very thin* alignment layers. The tilt angle ϑ_0 was measured optically; the spontaneous polarization P_s, rotational viscosity γ_φ, and specific conductivity σ were found from the magnitude and shape of the current oscillograms at different frequencies. We used the square-wave form of the external voltage (±12.5 V) for ϑ_0, P_s, γ_φ measurements and the triangular form (±14 V) for the σ determination.

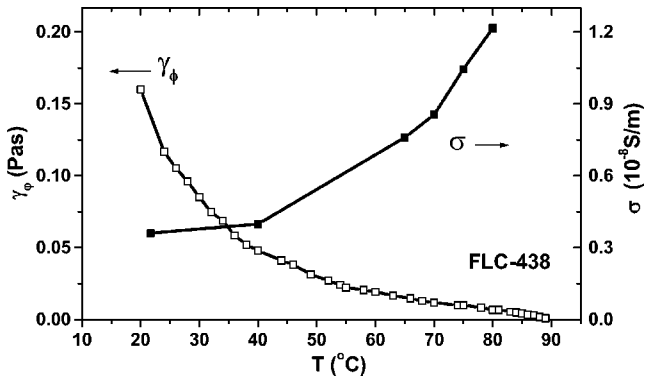

FIG. 2. Temperature dependencies of rotational viscosity γ_φ and dc conductivity σ of FLC-438.

As seen in the figures, our mixture has a temperature range of the ferroelectric phase from 10 °C to 90 °C. A wide temperature range is very important because the V-shape regime is mostly perspective for projection displays, which operate in the high intensity light beam, as a rule, at enhanced temperatures (about 40 °C and higher). Then, the mixture has a large tilt angle that is important for high optical transmission in the open states and large spontaneous polarization, see Fig. 1. The rotational viscosity of the mixture is rather low (Fig. 2), which is usually difficult to obtain for large tilt angle compounds. As we shall see later, a slightly enhanced specific conductivity of the mixture with respect to commercial FLCs is close to optimal for the high frequency V-shape switching. The optical anisotropy of the material at wavelength $\lambda = 633$ nm is $\Delta n \approx 0.20$–0.18 in a range of 25–60 °C. Finally, our mixture is well aligned by a conventional rubbing technique without the formation of chevrons.

2. Electro-optical cells

As modeling shows, thicker alignment layers promote high frequency hysteresis-free switching. However, thick polyimide layers due to their specific morphology often result in textures of insufficient quality. Therefore, for our cells we used glasses with double alignment layers at each indium-tin oxide (ITO) electrode. First thick (50–100 nm) Al_2O_3 layers have been evaporated, on top of which thin (10–20 nm) polyimide layers have been deposited by a spin-coating technique. For comparison, we also made cells with single thin (20–40 nm) polyimide layers deposited on each ITO electrode. In all cases, only one of the double or single alignment layers was rubbed in one direction while the other was not rubbed.

The gap between the glasses was fixed with calibrated glass balls spread onto the alignment layers from a solution of dimethylformamide using a spin-coating technique. As a rule, the area of the electrode overlapping was about 1 cm^2. The thickness of the liquid crystal layer d_{LC} is very important. In fact, there is a serious confinement on d_{LC} posed by optical requirements: the maximal optical transmission corresponds to the phase retardation $\delta = 2\pi\Delta n d/\lambda = \pi$. For $\Delta n \approx 0.2$, it means $d_{LC} \approx 1.5$ μm for the transmission regime and $d_{LC} \approx 0.75$ μm for the reflection (or double transmission) regime. In our experiments, we mostly use (0.7–1) -μm-thick cells.

B. V-shape electro-optical response

1. Form of the response

For the electro-optical V-shape regime, the so-called bookshelf geometry of the sandwich electro-optical cells is used with the smectic layer planes oriented perpendicular to the electrodes. The smectic layer normal coincides with the rubbing direction *z*. The director **n** in the bulk of the cell is tilted at an angle of ϑ_0 with respect to the electrode plane *z*, *y* and its projection onto the latter coincides with *z*. The polarizer and analyzer axes are installed parallel and perpendicular to the *z*, respectively. Therefore, in the field-off re-

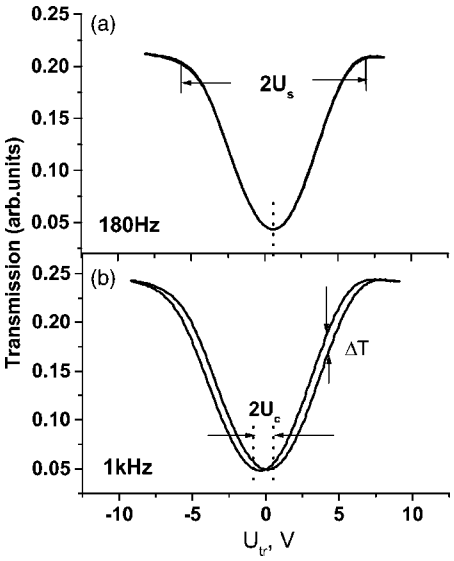

FIG. 3. Hysteresis free form (a) and normal hysteresis type (b) of the optical transmission curves taken for the same cell no. 1 at two different frequencies 180 Hz and 1 kHz, respectively.

gime, the optical transmission is minimal. When a positive or negative voltage is applied to the electrodes along the x axis, the polarization component P_x is switched up or down, while the director moves along the conical surface with its projection onto the z, y plane changing between the angles $\pm\vartheta_0$ with respect to z. Thus, the optical transmission in the field-on states is maximal in the two symmetric states with respect to the rubbing direction.

Two examples of the optical transmission curves are shown in Fig. 3. A cell was constructed for operation in the high frequency V-shape mode. The two curves differ by the frequency of an applied triangular waveform voltage U_{tr} of amplitude ± 10 V. The upper curve corresponds to the V-shape regime, because the frequency f of U_{tr} coincides with the so-called hysteresis inversion frequency ($f_i = 180$ Hz). This frequency is the principal property of the cell and depends on many parameters [10,11,14]. Strictly speaking, it is that single frequency at which one can observe the electro-optical hysteresis-free switching with zero coercive field and the V shape of the response. For $f > f_i$, we observe *normal* hysteresis when the director follows the external field with a time delay. This case is shown in Fig. 3(b) ($f = 1$ kHz); here the form of the curve resembles rather letter W with a finite coercive voltage U_c. For $f < f_i$, we observe the so-called *abnormal* hysteresis when the director goes ahead of the driving voltage U_{tr} (but, of course, behind the internal field depending on the capacitance of alignment layers). At $f = f_i$, the hysteresis on the external voltage scale disappears ($U_c = 0$).

The thickness of the FLC layer plays the key role in the high frequency hysteresis-free switching. Early experiments made on the wedge-shape cells [15] revealed a maximum of f_i at $d_{LC} \approx 0.8$–1 μm, by chance very close to the thickness of the optimum optical transmission. Figure 3 corresponds to cell no. 1 with $d_{LC} = 0.85$ μm and rather thick alignment layers (70 nm of Al_2O_3 plus 20 nm of PI on each electrode).

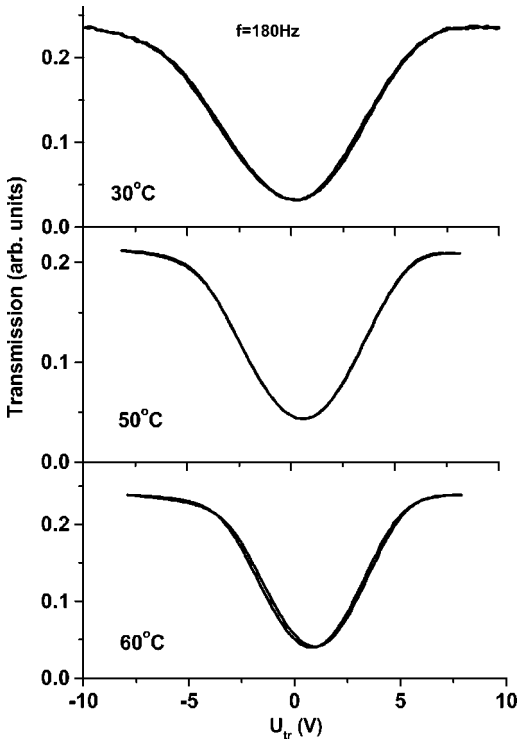

FIG. 4. Voltage dependencies of the optical transmission taken for the same FLC cell at three different temperatures $T = 30$, 50 and 60 °C (cell no. 1). (Note that the curves are shifted to the right from the zero field point, especially at increased T. This effect comes in from the intrinsic asymmetry of our cell with only one electrode rubbed. The latter may cause a dependence of FLC conductivity on field polarity due, e.g., to asymmetric charge injection processes.)

For practical purposes, it is not sufficient to have zero coercive voltage at $f = f_i$. To provide many levels of the gray scale, the transmission for the up and down scans of the voltage should follow the same curve for all voltage values. Figure 3(a) is a very good example: we specially selected a very thin line on the graph to show that the curve is not doubled. In addition, the coercive field in our cells weakly depends on frequency: an even six-times difference between f and f_i in Fig. 3(b) results in a very small value of $U_c \approx 200$ mV.

Another parameter important for the gray scale realization is the depth of the transmission minimum, which is necessary for a large dynamic range and a high contrast ($K = T_{max}/T_{min}$) of the response. Our computer modeling of the electro-optical switching of a cell with the bookshelf structure free of defects and aligning layers of uniform thickness shows that the contrast is only limited by the quality of polarizers. In experiment, the dynamic contrast is low ($K \approx 5$ in Figs. 3 and 4) while the same cells show the static, field-off contrast of about 100. The microscope observation of the texture without applied field reveals fine focal-conic defects responsible for this static contrast. We believe that these defects originate from small irregularities in the thickness of the aligning layers. Unfortunately, in the field-on, dynamic regime *the same defects* become much brighter under a microscope and reduce optical contrast.

The reason is clear from the physics of the process: any fluctuations in the thickness of the aligning layers produce

fluctuations of the voltage on the FLC layer that control the speed of the polarization and the director switching. At a place with thinner alignment layers, the internal field on the FLC is higher and the switching is faster. Therefore, the FLC director at that place goes ahead of the director at a neighbor place where the alignment layers are thicker, and a gradient of the director orientation appears at the boundary between the two places. This "dynamic director gradient" causes rather strong light scattering and increases T_{min}. Such scattering is an intrinsic feature of the high frequency hysteresis-free switching for two reasons: (i) generally, in the hysteresis-free regime, the internal field on FLC is small (see Sec. III A) and sensitive to any fluctuations; (ii) in the case of the high frequency effect, we inevitably have thick aligning layers and relatively thin FLC layers so the voltage fluctuations on an FLC layer are especially large. Our experiments show that with thick polyimide layers (single, without Al_2O_3), the high frequency V-shape effect is almost impossible to observe due to a poor contrast. Therefore, in order to increase the contrast, the technology of alignment layers has to be improved further.

With increasing U_{tr}, the transmission reaches saturation. The saturation voltage U_s is another important parameter of the electro-optical cells. The double saturation voltage is marked by arrows in Fig. 3(a). The requirements for a high inversion frequency and a low saturation voltage are to some extent contradictory, therefore a compromise should always be found.

2. Temperature dependence of f_i and U_s

Figure 4 shows examples of the electro-optical response at the same frequency ($f=180$ Hz) but at three different temperatures. The central curve taken at $T=50$ °C manifests the hysteresis-free switching. It is the same curve shown in Fig. 3(a). For temperatures $T=30$ °C and 60 °C, the inversion frequency is 70 and 500 Hz, respectively. Therefore, in both cases, at $f=180$ Hz there is a hysteresis in switching (normal at 30 °C and abnormal at 60 °C), although the coercive voltage is so small (about 10 mV) that the top and bottom lines in Fig. 4 are only slightly broadened. This is a specific feature of thin electro-optical cells. The temperature dependencies of both the inversion frequency and saturation voltage are shown in Fig. 5 for the same cell no. 1. Some difference in f_i in Figs. 4 and 5 is accounted for by a small variation of the cell thickness over the cell area about 1 cm^2 probed by a laser beam of about 3 mm in diameter. With increasing temperature, the inversion frequency increases dramatically and reaches a value as high as 1 kHz (at 75 °C), never reported before. The main reasons are a decrease in viscosity and an increase in conductivity of the substance. The saturation voltage decreases with temperature from 8.5 to 4 V (Fig. 5). For the microdisplays operating at enhanced temperature, both high f_i and low U_s are favorable factors. In addition, the cell thickness of 0.85 μm provides almost optimum optical transmission for the display operation in the reflection mode.

3. Alignment layers and saturation field

For a cell no. 2 with the same d_{LC} and thinner alignment layers (50 nm of Al_2O_3 and 20 nm of PI at each electrode), f_i also increases with temperature reaching the maximum value of only 520 Hz at 75 °C. This is due to an increase in capacitance of the thinner alignment layers. Correspondingly U_s is lower than in Fig. 5 (from 4 V at 30 °C to 2 V at 75 °C). We have studied the dependence of saturation field E_s on the thickness of the alignment layers prepared solely with either alumina or polyimide. Figure 6 (left) shows two $E_s(d_{AL})$ curves measured at $T=25$ °C on the cells with fixed thickness of FLC layer $d_{LC}=0.7\mu$m and varied thickness d_{AL} of polyimide and Al_2O_3 alignment layers. The external voltage was also varied and the saturation voltage was found according to its definition illustrated by Fig. 3. Then, for convenience of interpretation, the saturation field $E_s=U_s/d_{LC}$ was plotted against d_{AL}.

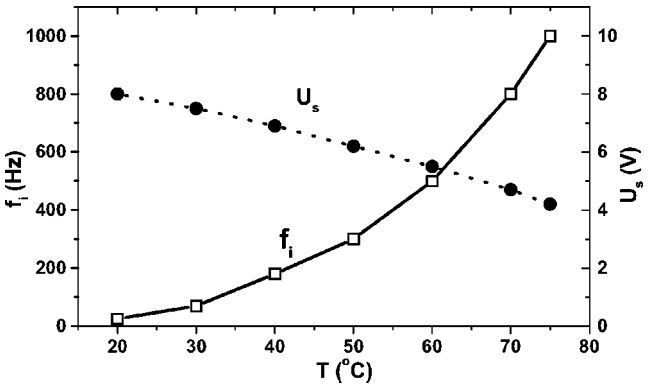

FIG. 5. Temperature dependencies of inversion frequency f_i and saturation voltage U_s for FLC cell no. 1.

At first glance, it would seem that E_s in Fig. 6 (left) depends on properties of the aligning material and the alumina layers are preferable for lowering E_s. However, due to a large difference in the dielectric constant of the two materials, the layers of $Al_2O_3(\varepsilon\approx 10)$ and PI ($\varepsilon\approx 3.4$) of equal thickness have different capacitance. In Fig. 6 (right), the same data for E_s are presented as functions of the inverse capacitance of the alignment layers. Now we can see that the two sets of

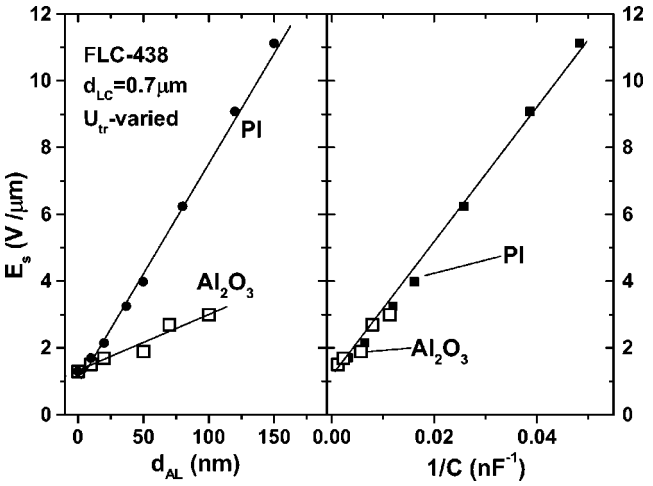

FIG. 6. Dependencies of the saturation field on the properties of Al_2O_3 and PI aligning layers presented on two different scales: alignment layer thickness d_{AL} (left) and inverse layer capacitance C^{-1} (right).

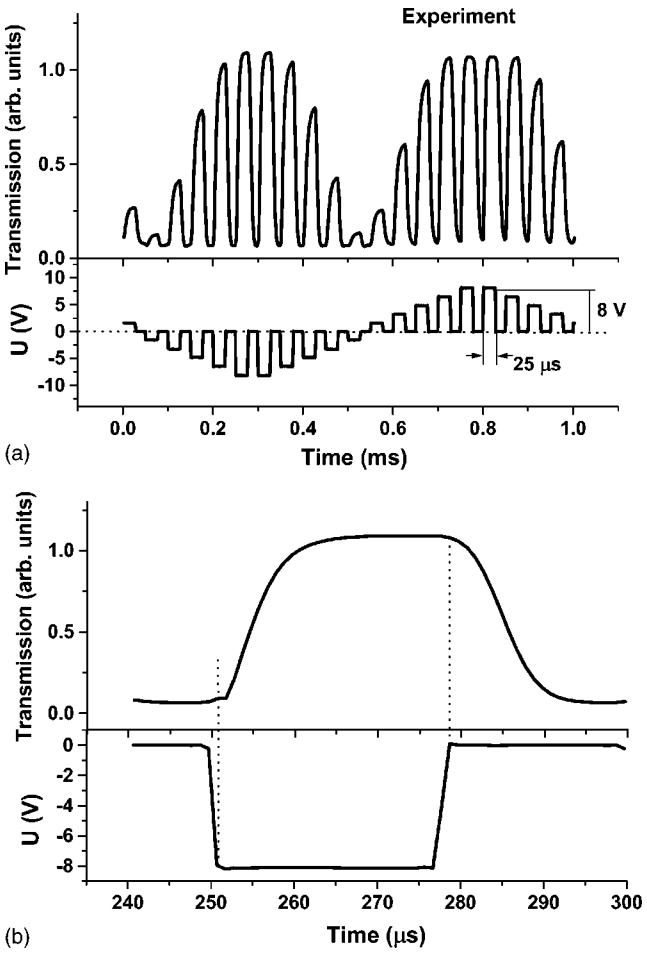

FIG. 7. (a) Forms of the voltage and the optical response of cell no. 3 showing a dependence of transmission on the pulse amplitude; (b) a blown part of the transmission and voltage curves showing the duration of the leading and trailing edges.

data fall onto the same line. This shows the principal importance of the global capacitance of the alignment layers independently of their thickness and dielectric constant or of whether the single or double layers are used. However, using thick alumina layers under thin PI layers is more profitable because, as AFM tests show, thin PI layers are more homogeneous and provide better quality of the FLC optical textures than thicker single PI layers of the same capacitance.

C. High frequency pulse response

Usual FLC cells manifest bistable switching and one should use pulses of opposite polarity to switch the optical transmission between the dark and bright states. However, our cells with high hysteresis inversion frequency manifest very particular response to a series of electric pulses of *the same polarity*. Such a response is shown in Fig. 7 and, to our knowledge, has never been observed yet. We have synthesized a sequence of 20 short (25 μs) rectangular pulses with the triangular envelope of 1 ms period. Such a voltage form allows us to observe simultaneously the electro-optical response to different voltage amplitudes.

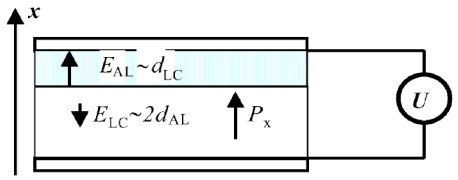

FIG. 8. (Color online) A model showing the appearance of the internal field opposite to the P_x direction at $U=0$ in the FLC layer previously polarized by high enough voltage U. The voltage source has a negligible internal resistance.

The experiment has again been done with a 0.75-μm-thick cell no. 3 having double alignment layers consisting of Al_2O_3 (70 nm) and PI (20–30 nm) at each electrode. The cell was kept at an enhanced temperature of 60 °C. At this temperature, the FLC viscosity is small ($\gamma_\varphi \approx 19$ mPa s) and the spontaneous polarization is still fairly large ($P_s \approx 65$ nC/cm^2) (see Figs. 1 and 2). Due to this and a small thickness of the cell ($d \approx 0.9$ μm together with alignment layers), its reaction time to the external voltage $U_p = 3$–8 V is quite short ($\tau_r \approx \gamma_\varphi d / P_s U_p \approx 9$–3 μs). For the optical transmission pulses, this corresponds to the leading edge duration of 14–6 μs. Indeed, at $U_p = 8$ V we observe in Fig. 7(b) the leading edge duration of about 7.5 μs that is very close to our estimation. Surprisingly, the trailing edge duration at $U_p = 0$ is almost the same (≈ 8.5 μs). The optical transmission and therefore the SmC* director relax very fast to the initial voltage-off state showing no bistability. This pure monostable switching may only be caused by a strong inverse internal field that appears after the trailing edges of the external pulses. In the next section, we shall model this process.

III. MODELLING AND DISCUSSION

The final aim of this section is to explain our experimental results quantitatively using the simulation technique developed earlier [10,12,14]. Our calculations will also show general tendencies as far as the high frequency V-shape switching is concerned. The consideration of the magnitude and the time dependence of the internal field in the FLC layer E_{LC} is a key point of our approach. Therefore, at first, we shall consider a very naive model that already describes some important features of the internal field.

A. Local field in ferroelectric liquid crystal layer (a simple electrostatic model)

A simplified double-layer electrostatic model is shown in Fig 8. In this model, we completely neglect conductivity of both the FLC and alignment layers and, instead of dynamic dielectric permittivity related to the P_s switching, we use a static dielectric constant ε_{LC}. The thicker layer mimics an FLC layer with the polarization component P_x directed up or down, depending on the applied field. The thinner layer mimics two insulating alignment layers with a total thickness $2d_{AL}$ and their capacitances connected in series. The equations for continuity of displacement D_x and distribution of voltages over the contour read

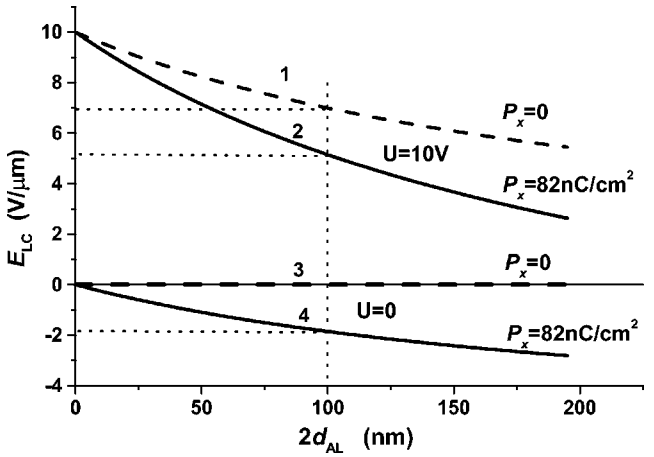

FIG. 9. Dependencies of the magnitude of the internal field in the FLC layer on PI alignment layer thickness d_{AL} for different external voltage U and FLC polarization component P_x [calculated with Eq. (2)].

$$\varepsilon_0\varepsilon_{AL}E_{AL} = \varepsilon_0\varepsilon_{LC}E_{LC} + P_x \equiv D_x,$$

$$2d_{AL}E_{AL} + d_{LC}E_{LC} = U. \tag{1}$$

From here, we can easily find the electric field in the two layers,

$$E_{LC} = \frac{\varepsilon_{AL}U - (P_x/\varepsilon_0)2d_{AL}}{(\varepsilon_{LC}2d_{AL} + \varepsilon_{AL}d_{LC})},$$

$$E_{AL} = \frac{\varepsilon_{LC}U + (P_x/\varepsilon_0)d_{LC}}{(\varepsilon_{LC}2d_{AL} + \varepsilon_{AL}d_{LC})}. \tag{2}$$

Due to the presence of polarization, the electric field exists in each layer even at $U=0$ and the two fields are opposite to each other, as shown in Fig. 8. At $U=0$, the internal field in the liquid crystal layer is always opposite to P_x and it is that internal field which is responsible for the hysteresis-free switching. The formula for E_{LC} can be presented in the "capacitance form" (S is the cell area),

$$E_{LC} = \frac{C_{2AL}C_{LC}(U/S - P_x/C_{2AL})}{\varepsilon_0\varepsilon_{LC}(C_{LC} + C_{2AL})}. \tag{3}$$

From this it is evident that the dielectric material of two alignment layers influences E_{LC} only implicitly through their equivalent capacitance C_{2AL} in agreement with our experimental data shown in Fig. 6. As to an FLC material, it does influence E_{LC} explicitly through ε_{LC} and P_x.

In Fig. 9, the internal field strength [Eq. (2)] is shown as a function of polyimide alignment layers thickness $2d_{AL}$ for a 1-μm-thick FLC layer with $\varepsilon_{LC}=15$. The static external voltage U is 10 V or zero. The x component $P_x = 82$ nC/cm^2 of the spontaneous polarization P_s corresponds to the polarization vector oriented along the cell normal while $P_x=0$ corresponds to the P_s orientation in the plane of the cell. For $U > 2d_{AL}P_x/\varepsilon_0\varepsilon_{AL}$, the sign of E_{LC} coincides with the sign of U. For small U, it is determined by the direction of P_x.

To be in accord with Fig. 9, we can predict how P_s would influence the internal field in an FLC layer in a dynamic regime when alignment layers are thick, e.g., $2d_{AL}=50\times 2 = 100$ nm (dotted vertical line in the figure). When a positive voltage pulse orients the spontaneous polarization up, the external field is not only reduced down to 7 V/μm due to a finite capacitance of the alignment layers (curve 1), but, in addition, it is dramatically screened by the polarization charges (down to 5.2 V, curve 2). When the external pulse is over, the capacitance of the alignment layers is still charged and creates a strong negative field in the FLC layer (-1.9 V/μm, see curve 4). This field would switch the P_s and the director back from the field-on state preventing bistability and hysteresis. This explains the monostable switching shown in Fig. 7.

When a triangular voltage is applied to a cell, the internal field effects become very important at low frequencies. In the case of nonconductive FLC due to the external field screening, the coercive field becomes very low and the hysteresis *almost* disappears. However, as shown in [16], to have an ideal hysteresis-free switching at a certain frequency (the change in the hysteresis direction at f_i, as seen in Figs. 3 and 4), the FLC must be conductive. This partially explains the strong temperature growth of f_i shown in Fig. 5, although a decrease in viscosity is also very important.

Curve 2 in Fig. 9 explains the growth of the saturation voltage E_s with alignment layer thickness. Since for a fixed voltage U_{tr} across the cell electrodes the internal field E_{LC} in the FLC layer is screened more and more with increasing d_{AL}, we have to increase U_{tr} to achieve the same optical effect. Thus, our experimental data can be understood qualitatively on the basis of the naive model. Now we shall look at the results of the much more advanced modeling procedure.

B. Modeling of the high frequency hysteresis-free switching

1. Parameters of the model

Our modeling procedure is described in detail in [13] and more briefly in [14]. In the same papers some examples are given. Here we shall focus on the modeling of hysteresis-free high frequency optical response. To this effect, we need to fix a large number of parameters, which can be divided in four groups: FLC material parameters; parameters of the cell construction; parameters determining the bookshelf, tilted, or chevron structure; and parameters of the applied field. The majority of these parameters are known from our experiment; the others, usually not of principal importance, were taken from the literature or reasonably estimated. Below, we present the full list of them with some comments. The values measured by us are left without comments.

(i) FLC parameters (at 35 °C): $P_s=84$ nC/cm^2; tilt angle $\vartheta_0=29°$; the components of the dielectric tensor $\varepsilon_\perp=7$, $\varepsilon_\parallel=17$ (calculated as $\varepsilon_\perp+\varepsilon_a$ with $\varepsilon_a=10$ taken from experiments with nematic phase of similar pyrimidine compounds); dc conductivity $\sigma=4\times10^{-9}$ S/m; refraction indices $n_\perp=1.53$, $n_\parallel=1.725$; rotational viscosity $\gamma_\varphi=\gamma_2\sin^2\vartheta_0 = 0.068$ Pa s (i.e., $\gamma_2=0.31$ Pa s; the other two components of the viscosity tensor related to the tilt angle relaxation [1]

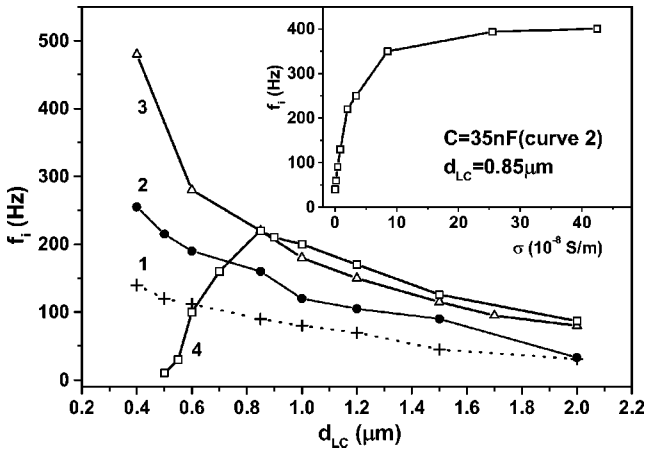

FIG. 10. Calculated dependencies of hysteresis inversion frequency on FLC layer thickness for different FLC conductivity σ and capacitance of alignment layers C. Curve 1 is calculated for the experimental values of $\sigma=4\times10^{-9}$ S/m and $C=35$ nF for cell no. 1; curves 2–4 are calculated for enhanced FLC conductivity $\sigma=2\times10^{-8}$ S/m and varied capacitance: $C=50$ nF (curve 2), 35 nF (curve 3), and 20 nF (curve 4). Inset: Hysteresis inversion frequency as a function of FLC specific conductivity for $d_{LC}=0.85$ μm and $C=35$ nF. For other parameters, see the text (Sec. III B 1).

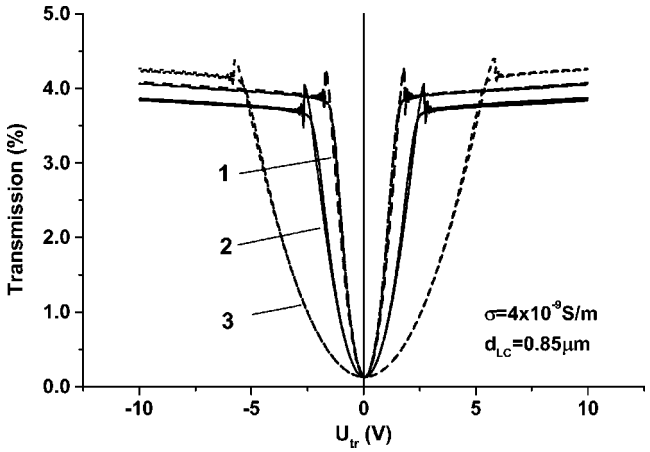

FIG. 11. Calculated voltage dependence of the optical transmission for $d_{LC}=0.85$ μm, conductivity $\sigma=4\times10^{-9}$ S/m, and different capacitance of alignment layers C. All curves are taken at the hysteresis inversion frequency. Curve 1: $C=50$ nF, $f_i=68$ Hz; curve 2: $C=35$ nF, $f_i=90$ Hz; curve 3: $C=20$ nF, $f_i=110$ Hz. [Notes: (a) Small spikes on the transmission curves near the saturation voltage are the artifacts resulting from the fast calculation mode. They can be easily eliminated by increasing the number of the x points along the cell normal, but this would dramatically increase the calculation time. (b) In our modeling, the properties of polarizers are considered to be close to those of typical film polarizers used in displays, which determine the minimum transmission of 0.13%.]

were taken an order of magnitude larger than γ_2, namely $\gamma_{1,3}=3$ Pa s); nematiclike elastic moduli, not normalized by $\sin^2\vartheta_0$, namely $K_{1,2,3}=10$, 3, and 3 pN (the order of magnitude was taken by analogy with nematics having large orientational order parameter); compressibility modulus $K_4=5$ MPa measured on similar mixture [14]; helical pitch $p=0.2$ μm.

(ii) FLC layer thickness $d_{LC}=0.85$ μm or varied, cell area 1 cm^2, capacitance of aligning layers $C=35$ nF/cm^2 or varied, conductivity of aligning layers $G_{AL}=0.005$ μS (negligible), cell electrode resistance 0.2kΩ.

(iii) Cell normal is along x, the bookshelf geometry with the smectic layer normal along z, easy axis **h** is oriented along z and forms a pretilt angle $\vartheta_s=4°$ with respect to both substrates (typical of polyimide), nematiclike quadrupolar anchoring energies are $W_z=0.1$ mJ/m^2 (zenithal) and $W_a=0.05$ mJ/m^2 (azimuthal), polar anchoring is neglected (W_z and W_a are taken assumed from analogy with nematics)

(iv) Triangular form applied voltage with amplitude ±10 V (if not said specifically).

2. Search for the highest possible inversion frequency

Trying to find the condition for maximum f_i at a given temperature (35 °C), we may vary only a limited number of parameters. The most important of them are the thickness of a liquid crystal layer, the capacitance of aligning layers, and the conductivity of a liquid crystal. In experiment, the latter can be varied by doping FLCs with conductive additives [16].

The main plot of Fig. 10 shows several important curves. Curve 1 is calculated with exactly the same set of parameters mentioned above. We have obtained a monotonic increase in f_i down to very small thickness of FLC layers. For $d_{LC}=0.85$ μm, the hysteresis inversion frequency is 90 Hz. This value is obtained with a capacitance of alignment layers of $C=35$ nF/cm^2 found from the measured thickness of a pair of Al_2O_3 (70 nm) and PI (20 nm) double layers. The calculated value should be compared with the experimental value of f_i at 35 °C, which varies in the range of 70–130 Hz for different 0.85-μm-thick cells. Note that upon the calculations, only one parameter was fitted: we noticed that a three-times increase of the splay elastic modulus K_1 with respect to the twist K_2 and bend K_3 elastic moduli results in a two-times increase in f_i. This anisotropy also improves the V shape of the transmission curve (no curve doubling with increasing voltage), simultaneously reducing the transmission maximum by a factor of 1.5. This is accounted for by the somewhat incomplete director switching in the material with enhanced anisotropy of K_i. Unfortunately, we are not aware with any data on the anisotropy of elastic moduli in the SmC^* phase.

Varying the alignment layer thickness, i.e., their capacitance with fixed $d_{LC}=0.85$ μm, we can additionally change the inversion frequency from 68 Hz ($C=50$ nF) to 110 Hz ($C=20$ nF), see the corresponding oscillogram in Fig. 11. For thicker alignment layers (curve 3), the saturation voltage is, of course, larger (the curve is wider) because a considerable part of the external voltage drops on these layers.

The agreement with the experiment can be easily improved by a slight increase in FLC dc conductivity σ. In fact, the inversion frequency is very sensitive to σ, as seen from the inset to Fig. 10. With the same thickness $d_{LC}=0.85$ μm, by variation of σ we can reach f_i as high as 400 Hz. If we fix the conductivity at a reasonable level, $\sigma=2\times10^{-8}$ S/m (the

value typical of nematics and easily achievable by slight FLC doping), we would have a family of three curves 2, 3, and 4 in Fig. 10 differing by alignment layer capacitance. For curves 1 and 3, the capacitance is the same, $C=35$ nF. We can see that with enhanced conductivity, f_i reaches the values of 220 Hz for $d_{LC}=0.85$ μm and even 480 Hz for thinner FLC layers ($T=35$ °C).

Generally f_i increases with decreasing FLC layer thickness (curves 1–3 in Fig. 10). However, for $C=20$ nF (two 77-nm-thick polyimide layers), the voltage on thin FLC layers ($d_{LC}<0.8$ μm, fixed $U_{tr}=10$ V) becomes too small and the switching regime changes. In this case, the saturation of the optical transmission is not observed and the inversion frequency dramatically drops down, see curve 4 in Fig. 10. This effect has also been observed in experiments on the wedge-type cells close to the wedge edge [15]. Another specific feature of very thin FLC layers is a dependence of inversion frequency on the dielectric anisotropy. Our calculations show that for $d_{LC}<0.6$ μm, large positive dielectric anisotropy (our case) substantially increases f_i. For instance, instead of the maximum value of $f_i=480$ Hz (curve 3, $\varepsilon_a=+10$), we would only have 300 Hz for $\varepsilon_a=0$.

As far as the saturation voltage is concerned, the modeling shows that U_s is almost independent of the FLC thickness. The reason has to do with a voltage dividing between the alignment layers and FLC layer. The electric field in FLC necessary for the optical transmission saturation is $E_s=U_{LC}/d_{LC}$. Therefore, with increasing d_{LC} at a fixed external voltage U_{tr}, the internal voltage U_{LC} is also growing and stabilizes E_s. In experiment, U_s slightly increases (by 20%) with a considerable decrease in FLC thickness from 2.4 μm down to 0.7 μm, therefore the calculated and experimental data agree. On the contrary, calculated U_s strongly grows with increasing the thickness of alignment layers (or a decrease in their capacitance). This is well seen in Fig. 11: with fixed $U_{tr}=10$ V, the saturation voltage increases from 2.1 V (curve 1, $C=50$ nF) to 3 V (curve 2, $C=35$ nF) and then to 6.1 V (curve 3, $C=20$ nF). In experiment, U_s is somewhat larger, for example in Fig. 4, for the same parameters $U_s\approx 5.6$ V($C\approx 35$ nF). This could be related to some inhomogeneity of the FLC texture. The modeling also shows that, in the ideal bookshelf texture placed between the ideal polarizers, the minimum transmission could be reduced to zero. This means that there is room for enhancement of the optical contrast of our cells.

In our experiments, we dealt only with bookshelf geometry; the chevrons were absent. However, Fig. 12 allows us to answer an important question: how important is a bookshelf structure for the high frequency hysteresis-free switching? We can model the tilted layer geometry and the symmetric chevrons with the apex in the middle of the FLC layer. In both cases, the smectic normal tilt corresponds to the thermodynamic angle ϑ_0. As seen from the figure, the three curves corresponding to the bookshelf (curve 1), tilted layer (curve 2), and chevron (curve 3) structures manifest a similar dependence of inversion frequency on the FLC layer thickness. Moreover, for the chevron structure f_i is maximal, however the transmission curve is more similar to letter M than to letter V; see the inset to Fig. 12. Of course, such a shape is related to the strong variation of the optical anisotropy due to a strong deviation of the smectic layer normal from the cell plane. Thus, such a curve is not suitable for the conventional V-shape regime. However, the inner part of the curve seems to be very interesting: the lines are ideally overlapped, very steep, linear, and show a small half-distance between the two maxima ($U_s^*=1.2$ V). Probably these properties of the chevron structure may also be useful for certain applications of the thresholdless switching.

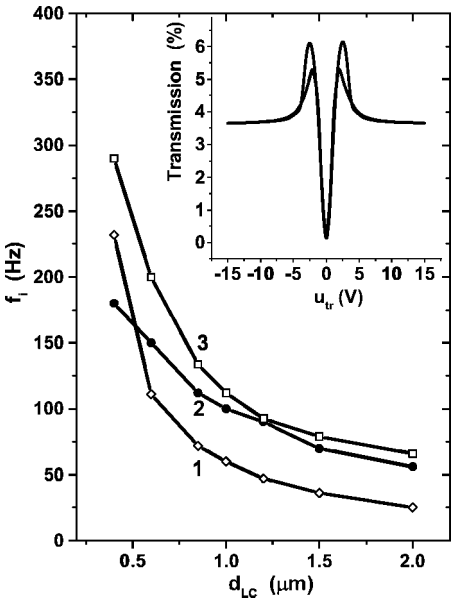

FIG. 12. Calculated dependencies of hysteresis inversion frequency on FLC layer thickness for the bookshelf (curve 1), tilted layer (curve 2), and chevron (curve 3) structures. Inset: Calculated voltage dependence of the optical transmission for a 0.85-μm-thick cell with a symmetric chevron structure. For other parameters, see the text (Sec. III B 1).

C. Modeling of the pulse electro-optical response

In this section, we show the results of modeling of our experimental data on the pulse electro-optical response obtained at $T=60$ °C for 0.75-μm-thick cell no. 3, see Fig. 7. Correspondingly, several temperature-dependent parameters from those listed in Sec. III B 1 were taken at 60 °C: $P_s=64$ nC/cm^2, $\vartheta_0=27.3°$, $\sigma=6.5\times10^{-9}$ S/m, $\gamma_\varphi=\gamma_2\sin^2\vartheta_0=19$ mPa s (i.e., $\gamma_2=0.094$, $\gamma_{1,3}=1$ Pa s), $K_{1,2,3}=6$, 2, and 2 pN, $K_4=2$ MPa, and capacitance of alignment layers C $=28$ nF. The voltage form is exactly the same as in the experiment. The result of our modeling is shown in Fig. 13. At the bottom of the figure, the external voltage form is shown; the maximum pulse amplitude is ±8 V. In the middle of the figure, we can see a form of the voltage on the FLC layer. In fact, it is markedly differentiated external voltage U_{ext}. For each positive pulse of U_{ext} (say 8 V), the internal voltage on the FLC layer U_{LC} has a positive part of a reduced amplitude ($\approx$4 V) followed by a negative pulse of even lower amplitude (about −1.5 or −2 V). However, this amplitude is sufficient for switching the director to the original state of the zero transmission (note that the polarizer is oriented along the rubbing direction and the analyzer is in the crossed po-

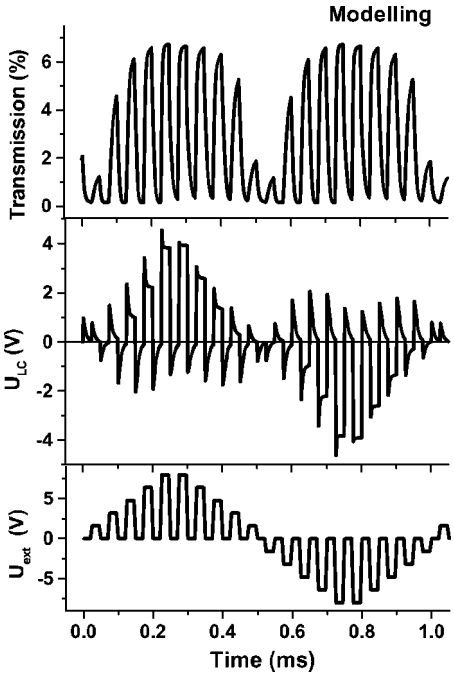

FIG. 13. Calculated time dependencies of the external pulse voltage U_{ext}, voltage on the FLC layer U_{LC}, and the optical transmission of a cell with parameters listed in the text.

sition). The calculated transmission curve shown on the top of the figure reproduces quite well the experimental curve shown in Fig. 7 without fitting parameters. In fact, the leading and trailing edges of the experimental curve are some 30% shorter than the calculated ones. This may come from certain errors in the experimental measurements of the FLC layer thickness (± 0.1 μm) and alignment layer thickness ($\pm 30\%$).

IV. CONCLUSION

In conclusion, we have demonstrated the high frequency hysteresis-free director switching and electro-optical V-shape effect in ferroelectric liquid crystal cells. A special FLC material has been designed and its basic properties (tilt angle, spontaneous polarization, rotational viscosity, and electric conductivity) have been measured over the entire range of the smectic-C^* phase. Upon variation of cell parameters (thickness of both the FLC and alignment layers), temperature, and external voltage, the frequency of the V-shape effect as high as 150–1000 Hz (in the temperature range 30–75 °C) has been found experimentally. In this case, the saturation voltage remains lower than 8 V. A quantitative interpretation of these results has been done using the modeling procedure developed earlier. The modeling has been performed with the experimental values of FLC material and cell parameters and has shown very good agreement with experiment. This approach allows further improvement of the performance of electro-optical FLC cells for the high frequency V-shape effect.

Resuming our earlier results [10,12–16] and the present discussion of the inversion frequency f_i, we may state that in order to have high frequency hysteresis-free switching in FLC cells, we should (i) provide a fast response of an FLC material to an applied field by increasing the P_s/γ_φ ratio; (ii) enhance conductivity of the FLC layer and not use conductive aligning layers; (iii) use materials with enhanced anisotropy of elasticity, $K_{11} > K_{22} = K_{33}$, and enhanced positive dielectric anisotropy; (iv) reduce the thickness of the FLC layer down to the value still sufficient for high optical transmission in the on-state; (v) decrease the capacitance of alignment layers by increasing their thickness and decreasing their dielectric constant; (vi) use very uniform alignment layers providing bookshelf structure completely free of defects; and (vii) use symmetric chevron structures for certain applications of high frequency thresholdless switching.

ACKNOWLEDGMENTS

The authors are grateful to DFG and DLR/BMBF (Germany) for the support of the German-Russian collaboration. L.M.B. and S.P.P. acknowledge the financial support from the Russian Federation for Basic Research (Grants No. 0302-17288 and No. 0402-16466). S.P.P. is also grateful to the Russian Science Support Foundation.

[1] S. T. Lagerwall, *Ferroelectric and Antiferroelectric Liquid Crystals* (Wiley-VCH, Weinheim, 1999), p. 390.
[2] N. A. Clark and S. T. Lagerwall, Appl. Phys. Lett. **36**, 899 (1980).
[3] S. Inui, N. Iimura, T. Suzuki, H. Iwane, K. Miyachi, Y. Takanishi, and A. Fukuda, J. Mater. Chem. **6**, 671 (1996).
[4] A. Chandani, Y. Cui, S. S. Seomun, Y. Takanishi, K. Ishikawa, H. Takezoe, and A. Fukuda, Liq. Cryst. **26**, 151 (1999); **26**, 167 (1999).
[5] N. A. Clark, D. Coleman, and J. E. Maclennan, Liq. Cryst. **27**, 985 (2000).
[6] N. J. Mottram and S. J. Elston, Phys. Rev. E **62**, 6787 (2000).
[7] Yu. Panarin, V. Panov, O. E. Kalinovskaya, and J. K. Vij, Ferroelectrics **246**, 35 (2000).
[8] M. Čopič, J. E. Maclennan, and N. Clark, Phys. Rev. E **63**, 031703 (2001).
[9] S. S. Seomun, V. P. Panov, J. K. Vij, A. Fukuda, and J. M. Oton, Phys. Rev. E **64**, 040701(R) (2001).
[10] L. M. Blinov, E. P. Pozhidaev, F. V. Podgornov, S. A. Pikin, S. P. Palto, A. Sinha, A. Yasuda, S. Hashimoto, and W. Haase, Phys. Rev. E **66**, 021701 (2002).
[11] M. Čopič, J. E. Maclennan, and N. Clark, Phys. Rev. E **65**, 021708 (2002).
[12] L. M. Blinov, S. P. Palto, A. L. Andreev, E. P. Pozhidaev, F. V. Podgornov, and W. Haase, Mol. Cryst. Liq. Cryst. **410**, 105 (2004).
[13] S. P. Palto, Kristallografiya **48**, 145 (2003) [Crystallogr. Rep.

48, 124 (2003)].
[14] S. P. Palto, F. V. Podgornov, W. Haase, and L. M. Blinov, Mol. Cryst. Liq. Cryst. **410**, 95 (2004).
[15] W. Haase, S. A. Pikin, F. V. Podgornov, E. P. Pozhidaev, H. Moritake, and A. D. L. Chandani Perera, Proc. SPIE **5003**, 51 (2003).
[16] L. M. Blinov, S. P. Palto, F. V. Podgornov, H. Moritake, and W. Haase, Liq. Cryst. **31**, 61 (2004).